AIAA JOURNAL
Vol. 35, No. 8, August 1997

Geometrically Nonlinear Theory of Initially Imperfect Sandwich Curved Panels Incorporating Nonclassical Effects

Liviu Librescu* and Terry Hause†
Virginia Polytechnic Institute and State University, Blacksburg, Virginia 24061-0219
and
Charles J. Camarda‡
NASA Langley Research Center, Hampton, Virginia 23681-0001

A comprehensive geometrically nonlinear theory of initially imperfect doubly curved sandwich shells is developed. The theory encompasses sandwich structures with dissimilar face sheets constructed of laminate composites and with the core modeled as an orthotropic body featuring strong or soft behaviors. The theory includes the dynamic as well as the temperature and moisture effects. As a special case, a range of related applications of the theory of sandwich shells with soft core are presented. These involve the buckling and postbuckling of flat and circular cylindrical shells compressed by uniaxially edge loads, and the influence played in this respect by a number of geometrical and physical parameters is highlighted. Also contained are comparisons of buckling results obtained in the context of the present theoretical model with the ones obtained experimentally, and reasonable agreements are reported.

Nomenclature

$A_{\omega\rho}$, $A^*_{\omega\rho}$	= stiffness quantities associated with the facings and their inverted counterparts, respectively
a	= the distance between the global midsurface and the midsurface of facings
$B_{\omega\rho}$, $D_{\omega\rho}$, $F_{\omega\rho}$	= stiffness quantities associated with the facings
C_1, C_2	= geometrical quantities [Eqs. (26)]
$c_{\alpha\beta}$	= two-dimensional permutation symbol
E_1, E_2	= in-plane Young's moduli
e_{ij}	= three-dimensional strain tensor
$\bar{G}_{13}$, $\bar{G}_{23}$	= transverse shear moduli of the core
$H_{\alpha\beta}$, $\hat{H}_{\alpha\beta}$, $L_{\alpha\beta}$	= modified stress couple measures [Eqs. (19)]
h, $\bar{h}$, H	= thickness of the facings, that of the core, and the total thickness of the structure, respectively
k, k_1	= measures of transverse shear flexibility for the entire structure in the case of isotropic faces and transversely isotropic core and of orthotropic faces and orthotropic core, respectively
L_1, L_2	= length and width of the flat/curved panel
$M_{\alpha\beta}$, $N_{\alpha\beta}$	= stress couples and stress resultants measures [Eqs. (20) and (21)]
$\bar{N}_{13}$, $\bar{N}_{23}$	= transverse shear stress resultants associated with the core
$\mathcal{N}$, $\mathcal{N}$	= dimensionless form of the normal edge loads
Q_{ij}, $\hat{Q}_{ij}$	= elastic moduli and their modified counterparts, respectively
$\bar{Q}_{44}$, $\bar{Q}_{55}$	= transverse shear moduli associated with the core
q_3	= transverse load
R_1, R_2	= principal radii of curvature of the global midsurface
r	= dimensionless thickness ratio
S_{ij}	= second Piola–Kirchhoff stress tensor
v_3, $\mathring{v}_3$	= transversal deflection and initial geometric imperfection, respectively
x_α, x_3	= tangential and the thicknesswise coordinate, respectively
α^2	= measure of the curvature of the circular cylindrical panel
Δ_1	= end-shortening in the x_1 direction
δ_{mn}, $\mathring{\delta}_{mn}$	= dimensionless amplitude of transverse deflection and initial geometric imperfections, respectively
ϵ_{ij}	= two-dimensional strain measures
$\hat{\lambda}_{ij}$, $\hat{\mu}_{ij}$	= reduced thermal expansion and moisture swelling coefficients, respectively
λ_m, μ_n	= $m\pi/L_1$, $n\pi/L_2$
ξ_α, η_α	= two-dimensional tangential displacement measures [Eqs. (8)]
ϕ	= Airy's potential function
ψ	= panel aspect ratio

Subscripts, Superscripts, and Underscoring Signs

$(\ )_f$, $(\ )_c$	= quantities associated with the face and core layers, respectively
$(\ )_{,i}$	= $\partial(\ )/\partial x_i$
$(\ )_{,n}$, $(\ )_{,t}$	= derivitives of $(\ )$ with respect to the coordinates normal and tangential to an edge, respectively
$(\ )'$, $(\ )''$, $\bar{(\ )}$	= quantities affiliated with the bottom, upper, and core layers, respectively
$\underset{\sim}{(\ )}$	= prescribed quantity

Introduction

THE next generation of supersonic/hypersonic flight and launch vehicles has to be designed to meet increasingly stringent performance requirements. They are likely to operate in hostile environments consisting of high temperature, moisture, and pressure fields. Moreover, these vehicles will typically experience these loadings in a dynamic environment. Of great promise toward the successful solution of a number of technical challenges raised by the design of these advanced space vehicles is the ongoing integration in their construction of composite material systems. In this sense, the sandwich-type constructions can be viewed as a special type of laminated composite structures.

The sandwich structures encompass a number of properties of exceptional importance toward fulfillment of the high exigencies imposed upon these vehicles. Among others they feature 1) high bending stiffness characteristics with little resultant weight penalty, 2) a smoother aerodynamic surface in a higher-speed range, 3) excellent thermal and sound insulation and increased strength at elevated

---

Presented as Paper 96-1350 at the AIAA 37th Structures, Structural Dynamics, and Materials Conference, Salt Lake City, UT, April 15–17, 1996; received Aug. 21, 1996; revision received May 3, 1997; accepted for publication May 11, 1997.

*Professor, Department of Engineering Science and Mechanics.

†Research Assistant, Department of Engineering Science and Mechanics.

‡Head, Thermal Structures Branch; currently Astronaut, NASA Johnson Space Center, Houston, TX 77058-3696. Associate Fellow AIAA.

temperatures, and 4) a longer operational time as compared with stiffened-reinforced structures that are weakened by the appearance of stress concentration.

Characteristic for the standard sandwich-type constructions composed traditionally of a thick core and two identical metallic thin face layers is their capacity to carry the various load components in a specialized way; in the sense that the bending moments are predominately taken up as tensile and compressive stresses in the faces, whereas the core is designated to carry transverse forces in terms of shear stresses. The possibility to design the faces and the core according to their specific needs yields the high overall stiffness and strength per unit weight of such constructions.

However, exact separation of tasks, as considered in their classical modelings, becomes questionable when dealing with advanced sandwich-type constructions. Increasing core stiffness can significantly contribute to the overall membrane and bending stiffness while the increasing integration of anisotropic composite materials in the relatively thick face layers should be followed by the incorporation of transverse shear effects in the faces. Moreover, as the face layers of advanced sandwich structures are likely to be composed of anisotropic fiber-reinforced laminated composites featuring symmetry/nonsymmetry properties with respect to their own midsurfaces and to that of the core layer, additional couplings are induced whose implications have to be emphasized. Due to all of these new features, to predict accurately their load-carrying capacity and static/dynamic response behavior, more advanced models of sandwich-type constructions are needed.

The goal of the present paper is to develop such a comprehensive sandwich-type structural model capable of providing accurate predictions of its static and dynamic behavior under complex mechanical and thermal loads in the pre- and postbuckling ranges. Specialized variants of the obtained equations are used to study the buckling/postbuckling behavior of compressively loaded flat/curved sandwich panels, and comparisons with available experimental data are recorded.

In spite of the considerable importance of this problem, a modest amount of related work can be found in the literature. Here, only a few papers that are pertinent to the present developments, such as Refs. 1–5 and Refs. 6–9, which are devoted to the theory of flat and curved sandwich constructions, respectively, are mentioned. For a comprehensive and most recent survey of the status, achievements, and trends in the modeling of sandwich plates and shells, see Ref. 10.

Basic Assumptions

The global middle surface of the structure selected to coincide with that of the core layer is referred to as a curvilinear and orthogonal coordinate system x_α ($\alpha = 1, 2$). The transverse normal coordinate x_3 is considered positive when measured in the direction of the downward normal to the midsurface. We also assume that the uniform thickness of the core is $2\bar{h}$, whereas those of the bottom and upper faces are h' and h'', respectively. As a result, $-(\bar{h} + h'') \le x_3 \le (\bar{h} + h')$, and $H(\equiv 2\bar{h} + h' + h'')$ denotes the total thickness of the structure. For the sake of identification, unless otherwise stated, the quantities associated with the core will be accompanied by a superposed bar, whereas those associated with the lower and upper faces will be accompanied by single and double primes, respectively, placed on the right or left of the respective quantity. In the forthcoming developments, in addition to the (global) midsurface of the structure, the midsurfaces of the upper and bottom composite facings will also be considered in the analysis.

The geometrically nonlinear theory of doubly curved sandwich shells developed herein is based on a number of assumptions: 1) The face sheets are constructed of a number of orthotropic material layers, the axes of orthotropy of the individual plies, being not necessarily coincident with the geometrical axes x_α of the structure. 2) The core material features orthotropic properties, the axes of orthotropy being parallel to the geometrical axes x_α. It is also assumed that the thickness of the core is much larger than the thicknesses of the face sheets, i.e., $2\bar{h} \gg h', h''$. 3) The developed theory encompasses the cases of both weak and strong core sandwich structures. In the former case, the core is capable of carrying transverse shear stresses only, whereas in the latter one, the core can carry both tangential and transverse shear stresses. The method enabling one to obtain the equations of sandwich shells with weak core as a special case of those associated with strong core is properly indicated. 4) A perfect bonding between the face sheets and between the faces and the core is postulated. 5) The core and face layers are incompressible in transverse normal direction. 6) The principles of shallow shell theory are applied in this study.

Displacement Field

The three-dimensional displacement field in the facings and core is represented as follows.

For the bottom facings ($\bar{h} \le x_3 \le \bar{h} + h'$):

$$ {}'V_1(x_\alpha, x_3) = {}'V_1^0(x_\alpha) + (x_3 - a')\psi_1'(x_\alpha) \tag{1a} $$

$$ {}'V_2(x_\alpha, x_3) = {}'V_2^0(x_\alpha) + (x_3 - a')\psi_2'(x_\alpha) \tag{1b} $$

$$ {}'V_3(x_\alpha, x_3) = {}'v_3(x_\alpha) \tag{1c} $$

For the core layer ($-\bar{h} \le x_3 \le \bar{h}$):

$$ \bar{V}_1(x_\alpha, x_3) = \bar{V}_1^0(x_\alpha) + x_3\bar{\psi}_1(x_\alpha) \tag{2a} $$

$$ \bar{V}_2(x_\alpha, x_3) = \bar{V}_2^0(x_\alpha) + x_3\bar{\psi}_2(x_\alpha) \tag{2b} $$

$$ \bar{V}_3(x_\alpha, x_3) = \bar{v}_3(x_\alpha) \tag{2c} $$

For the top facing ($-\bar{h} - h'' \le x_3 \le -\bar{h}$):

$$ {}''V_1(x_\alpha, x_3) = {}''V_1^0(x_\alpha) + (x_3 + a'')\psi_1''(x_\alpha) \tag{3a} $$

$$ {}''V_2(x_\alpha, x_3) = {}''V_2^0(x_\alpha) + (x_3 + a'')\psi_2''(x_\alpha) \tag{3b} $$

$$ {}''V_3(x_\alpha, x_3) = {}''v_3(x_\alpha) \tag{3c} $$

In these equations, ${}'V_\alpha^0$, ψ_α'; ${}''V_\alpha^0$, ψ_α''; and $\bar{V}_\alpha^0$, $\bar{\psi}_\alpha$ denote the tangential displacements of the points of the midsurface and the shear angle rotations of the bottom and upper face sheets and of the core layer, respectively, whereas $a'(\equiv \bar{h} + h'/2)$ and $a''(\equiv \bar{h} + h''/2)$ denote the distances between the global midsurface and the midsurfaces of the bottom and top facings, respectively. Needless to say, in the dynamic case, all the displacement quantities as well as the strain and stress measures (to be defined later) are functions of the time variable, as well.

Fulfillment of the kinematic continuity conditions at the interfaces between the core and facings, from Eqs. (1–3) and in the light of assumption 5, implying

$$ {}'v_3 = {}''v_3 = \bar{v}_3 \equiv v_3 \tag{4} $$

the three-dimensional displacement components result as follows.

For $\bar{h} \le x_3 \le \bar{h} + h'$:

$$ {}'V_1(x_\alpha, x_3) = \xi_1(x_\alpha) + \eta_1(x_\alpha) + (x_3 - a')\,{}'\psi_1(x_\alpha) \tag{5a} $$

$$ {}'V_2(x_\alpha, x_3) = \xi_2(x_\alpha) + \eta_2(x_\alpha) + (x_3 - a')\,{}'\psi_2(x_\alpha) \tag{5b} $$

$$ {}'V_3(x_\alpha, x_3) = v_3(x_\alpha) \tag{5c} $$

For $-\bar{h} \le x_3 \le \bar{h}$:

$$ \bar{V}_1(x_\alpha, x_3) = \xi_1(x_\alpha) - \tfrac{1}{4}[{}'h\,\psi_1'(x_\alpha) - {}''h\,\psi_1''(x_\alpha)] + (x_3/\bar{h})\left\{\eta_1(x_\alpha) - \tfrac{1}{4}[{}'h\,\psi_1'(x_\alpha) + {}''h\,\psi_1''(x_\alpha)]\right\} \tag{6a} $$

$$ \bar{V}_2(x_\alpha, x_3) = \xi_2(x_\alpha) - \tfrac{1}{4}[{}'h\,\psi_2'(x_\alpha) + {}''h\,\psi_2''(x_\alpha)] + (x_3/\bar{h})\left\{\eta_2(x_2) - \tfrac{1}{4}[{}'h\,\psi_2'(x_\alpha) + {}''h\,\psi_2''(x_\alpha)]\right\} \tag{6b} $$

$$ \bar{V}_3(x_\alpha, x_3) = v_3(x_\alpha) \tag{6c} $$

For $-\bar{h} - h'' \le x_3 \le \bar{h}$:

$$ {}''V_1(x_\alpha, x_3) = \xi_1(x_\alpha) - \eta_1(x_\alpha) + (x_3 + a'')\,{}''\psi_1(x_\alpha) \tag{7a} $$

$$ {}''V_2(x_\alpha, x_3) = \xi_2(x_\alpha) - \eta_2(x_\alpha) + (x_3 + a'')\,{}''\psi_2(x_\alpha) \tag{7b} $$

$$ {}''V_3(x_\alpha, x_3) = v_3(x_\alpha) \tag{7c} $$

In these equations, the new two-dimensional tangential displacement measures $\xi_\alpha(x_1, x_2)$ and $\eta_\alpha(x_1, x_2)$ are defined as

$$\xi_1 = \frac{{}'V_1^0 + {}''V_1^0}{2} \tag{8a}$$

$$\eta_1 = \frac{{}'V_1^0 - {}''V_1^0}{2} \tag{8b}$$

$$\xi_2 = \frac{{}'V_2^0 + {}''V_2^0}{2} \tag{8c}$$

$$\eta_2 = \frac{{}'V_2^0 - {}''V_2^0}{2} \tag{8d}$$

Hence, the two-dimensional displacement measures reduce to nine functions, namely, ξ_1, ξ_2, η_1, η_2, v_3, ${}'\psi_1$, ${}'\psi_2$, ${}''\psi_1$, and ${}''\psi_2$. Assuming that the structure also features a stress-free initial geometric imperfection $\mathring{V}_3[\equiv \mathring{v}_3(x_\alpha)]$ and adopting the concept of small strains and moderately small rotations,[11] the three-dimensional strain-displacement relationship in Lagrangian description is

$$2e_{ij} = V_{i\|j} + V_{j\|i} + V_{3\|i}V_{3\|j} + V_{3\|i}\mathring{V}_{3\|j} + \mathring{V}_{3\|i}V_{3\|j} \tag{9}$$

By convention, the transverse deflection is measured from the imperfect surface, in the positive, inward direction. In Eq. (9), $(\ )_{i\|j}$ denotes the covariant derivative with respect to the metric of the three-dimensional space. Using the relationships between covariant derivatives of space and surface tensors (see Refs. 5 and 12), from Eqs. (5–9) and consistent with the concept of shallow shells, the following strain distribution is obtained.

In the bottom facing ($\bar{h} \le x_3 \le \bar{h} + h'$):

$${}'e_{11} = {}'\varepsilon_{11} + (x_3 - a'){}'\kappa_{11} \tag{10a}$$

$${}'e_{22} = {}'\varepsilon_{22} + (x_3 - a'){}'\kappa_{22} \tag{10b}$$

$$2{}'e_{12} = {}'\gamma_{12} + (x_3 - a'){}'\kappa_{12} \tag{10c}$$

$$2{}'e_{13} = {}'\gamma_{13} \tag{10d}$$

$$2{}'e_{23} = {}'\gamma_{23} \tag{10e}$$

In the core layer ($-\bar{h} \le x_3 \le \bar{h}$):

$$\bar{e}_{11} = \bar{\varepsilon}_{11} + x_3\bar{\kappa}_{11} \tag{11a}$$

$$\bar{e}_{22} = \bar{\varepsilon}_{22} + x_3\bar{\kappa}_{22} \tag{11b}$$

$$2\bar{e}_{12} = \bar{\gamma}_{12} + x_3\bar{\kappa}_{12} \tag{11c}$$

$$2\bar{e}_{13} = \bar{\gamma}_{13} \tag{11d}$$

$$2\bar{e}_{23} = \bar{\gamma}_{23} \tag{11e}$$

In the upper facing ($-\bar{h} - h'' \le x_3 \le -\bar{h}$):

$${}''e_{11} = {}''\varepsilon_{11} + (x_3 + a''){}''\kappa_{11} \tag{12a}$$

$${}''e_{22} = {}''\varepsilon_{22} + (x_3 + a''){}''\kappa_{22} \tag{12b}$$

$$2{}''e_{12} = {}''\gamma_{12} + (x_3 + a''){}''\kappa_{12} \tag{12c}$$

$$2{}''e_{13} = {}''\gamma_{13} \tag{12d}$$

$$2{}''e_{23} = {}''\gamma_{23} \tag{12e}$$

In these equations, ε_{11}, ε_{22}, $\varepsilon_{12}(\equiv \gamma_{12}/2)$, $\varepsilon_{13}(\equiv \gamma_{13}/2)$, and $\varepsilon_{23}(\equiv \gamma_{23}/2)$ denote the two-dimensional tangential and the transverse shear strain measures, respectively. Their expressions in terms of the two-dimensional displacement measures are displayed in Appendix 1.

When the Love–Kirchhoff hypothesis is adopted for both the upper and bottom face sheets, Eqs. (5–7) should be specialized, in the sense of ${}'\psi_\alpha = {}''\psi_\alpha = -\partial v_3/\partial x_\alpha$.

Furthermore, for symmetric sandwich structures, one should consider

$$h' = h'' \equiv h \tag{13a}$$

$$a' = a''(\equiv a) = \bar{h} + h/2 \tag{13b}$$

For some other modeling issues related to the theory of sandwich plates, the reader is referred to Ref. 13.

Equations of Equilibrium/Motion and Boundary Conditions

The Hamilton variational principle is used to derive the equations of equilibrium/motion and the boundary conditions of the theory of shallow sandwich shells. This variational principle may be stated as

$$\delta J = \delta \int_{t_0}^{t_1} (U - W - T)\,\mathrm{d}t = 0 \tag{14}$$

where t_0 and t_1 are two arbitrary instants of time; U denotes the strain energy; W denotes the work done by surface tractions, edge loads, and body forces; T denotes the kinetic energy of the three-dimensional body of the sandwich structure; and δ denotes the variation operator.

For the various parts of the variational equation, we have

$$\delta U = \frac{1}{2}\int_\sigma \left[\int_{\bar{h}}^{\bar{h}+h'} {}'S_{ij}\,\delta{}'e_{ij} + \int_{-\bar{h}}^{+\bar{h}} \bar{S}_{ij}\,\delta\bar{e}_{ij} + \int_{-\bar{h}-h''}^{-\bar{h}} {}''S_{ij}\,\delta{}''e_{ij} \right] \mathrm{d}x_3\,\mathrm{d}\sigma \qquad (i,\ j = 1,\ 2,\ 3) \tag{15}$$

where the usual summation convention over a repeated index is employed; S_{ij} denotes the second Piola–Kirchhoff stress tensor and σ denotes the undeformed midsurface of the sandwich shell. In addition,

$$\int_{t_0}^{t_1} \delta T\,\mathrm{d}t = -\int_{t_0}^{t_1} \mathrm{d}t \left[\int_\sigma \int_{\bar{h}}^{\bar{h}+h'} {}'\rho \ddot{V}_i \delta V_i\,\mathrm{d}x_3 + \int_{-\bar{h}}^{\bar{h}} \bar{\rho}\ddot{V}_i\delta V_i\,\mathrm{d}x_3 + \int_{-\bar{h}-h''}^{-\bar{h}} {}''\rho\ddot{V}_i\delta V_i\,\mathrm{d}x_3 \right] \tag{16}$$

where it was considered that $\delta V_i = 0$ at $t = t_0$, t_1, and

$$\delta W = \int_\sigma \left[\int_{\bar{h}}^{\bar{h}+h'} {}'\rho H_i \delta V_i\,\mathrm{d}\sigma\mathrm{d}x_3 + \int_{-\bar{h}}^{\bar{h}} \bar{\rho} H_i\delta V_i\,\mathrm{d}\sigma\mathrm{d}x_3 + \int_{-\bar{h}-h''}^{-\bar{h}} {}''\rho H_i \delta V_i\,\mathrm{d}\sigma\mathrm{d}x_3 \right] + \int_{\Omega_s} \underset{\sim}{S}_i \delta V_i\,\mathrm{d}\Omega \tag{17}$$

In Eqs. (16) and (17), the superposed dots denote time derivatives, ρ denotes the mass density, $\underset{\sim}{S}_i = \underset{\sim}{S}_{ij}n_j$ are the components of the stress vector prescribed on the part Ω_s of the external boundary Ω, n_i denotes the components of the outward unit vector normal to Ω, and H_i denotes the components of the body force vector.

From Eq. (14), considered in conjunction with Eqs. (15–17), and with the strain-displacement relationships (10–12) (used as subsidiary conditions), carrying out the integration with respect to x_3 and integrating by parts wherever feasible, using the expression of global stress resultants and stress couples (to be defined later), and invoking the arbitrary and independent character of variations $\delta\xi_1$, $\delta\xi_2$, $\delta\eta_1$, $\delta\eta_2$, $\delta{}'\psi_1$, $\delta{}'\psi_2$, $\delta{}''\psi_1$, $\delta{}''\psi_2$, and δv_3, one derives the equations of equilibrium/motion and the boundary conditions. Upon retaining only the transversal load and transverse inertia terms, the equations of motion are

$$\delta\xi_1: N_{11,1} + N_{12,2} = 0 \tag{18a}$$

$$\delta\xi_2: N_{22,2} + N_{12,1} = 0 \tag{18b}$$

$$\delta\eta_1: L_{11,1} + L_{12,2} - \bar{N}_{13} = 0 \tag{18c}$$

$$\delta\eta_2:\ L_{22,2} + L_{12,1} - \bar{N}_{23} = 0 \tag{18d}$$

$$\delta\psi'_1:\ \hat{H}_{11,1} + \hat{H}_{12,2} + N'_{13} - (h'/4\bar{h})\bar{N}_{13} = 0 \tag{18e}$$

$$\delta\psi'_2:\ \hat{H}_{22,2} + \hat{H}_{12,1} + N'_{23} - (h'/4\bar{h})\bar{N}_{23} = 0 \tag{18f}$$

$$\delta\psi''_1:\ \hat{\hat{H}}_{11,1} + \hat{\hat{H}}_{12,2} + N''_{13} + (h''/4\bar{h})\bar{N}_{13} = 0 \tag{18g}$$

$$\delta\psi''_2:\ \hat{\hat{H}}_{22,2} + \hat{\hat{H}}_{12,1} + N''_{23} - (h''/4\bar{h})\bar{N}_{23} = 0 \tag{18h}$$

$$\begin{aligned}\delta v_3:\ & N_{11}(v_{3,11} + \mathring{v}_{3,11} + 1/R_1) + 2N_{12}(v_{3,12} + \mathring{v}_{3,12}) \\ & + N_{22}(v_{3,22} + \mathring{v}_{3,22} + 1/R_2) + N_{13,1} + N_{23,2} + q_3 - m_0\ddot{v}_3 = 0\end{aligned} \tag{18i}$$

In these equations, $1/R_1$ and $1/R_2$ denote the principal curvatures of the global middle surface, $(\ )_{,\alpha}[\equiv \partial(\ )/\partial x_\alpha]$ denotes the partial differentiation with respect to the surface coordinate x_α, q_3 is the distributed transversal load, and m_0 denotes the reduced mass per unit area of the shell midsurface. As concerns the global stress resultants and stress couples in terms of which Eqs. (18) are expressed, these are defined as

$$N_{11} = N'_{11} + \bar{N}_{11} + N''_{11} \qquad (1 \rightleftarrows 2) \tag{19a}$$

$$N_{12} = N'_{12} + \bar{N}_{12} + N''_{12} \tag{19b}$$

$$N_{13} = N'_{13} + \bar{N}_{13} + N''_{13} \qquad (1 \rightleftarrows 2) \tag{19c}$$

$$L_{11} = \bar{h}(N'_{11} - N''_{11}) + \bar{M}_{11} \qquad (1 \rightleftarrows 2) \tag{19d}$$

$$L_{12} = \bar{h}(N'_{12} - N''_{12}) + \bar{M}_{12} \tag{19e}$$

$$\hat{H}_{11} = (h'/4)(\bar{N}_{11} + \bar{M}_{11}/\bar{h}) - M'_{11} \qquad (1 \rightleftarrows 2) \tag{19f}$$

$$\hat{H}_{12} = (h'/4)(\bar{N}_{12} + \bar{M}_{12}/\bar{h}) - M'_{12} \tag{19g}$$

$$\hat{\hat{H}}_{11} = (h''/4)(\bar{N}_{11} - \bar{M}_{11}/\bar{h}) + M''_{11} \qquad (1 \rightleftarrows 2) \tag{19h}$$

$$\hat{\hat{H}}_{12} = (h''/4)(\bar{N}_{12} - \bar{M}_{12}/\bar{h}) + M''_{12} \tag{19i}$$

where the sign $(1 \rightleftarrows 2)$ indicates that the expressions of the stress resultants and stress couples not explicitly written can be obtained from the ones just displayed upon replacing subscript 1 by 2 and vice versa.

In Eqs. (19), consistent with the concept of shallow shell theory, the stress resultants and stress couples associated with the bottom facings and the core are, respectively,

$$\{N'_{\alpha\beta}, M'_{\alpha\beta}\} = \sum_{k=1}^{n'} \int_{(x_3)_{k-1}}^{(x_3)_k} (S'_{\alpha\beta})_k \{1, x_3 - a'\}\,\mathrm{d}x_3 \tag{20a}$$

$$N'_{\alpha 3} = \sum_{k=1}^{n'} \int_{(x_3)_{k-1}}^{(x_3)_k} (S'_{\alpha 3})_k\,\mathrm{d}x_3 \qquad (\alpha, \beta = 1, 2) \tag{20b}$$

and

$$\{\bar{N}_{\alpha\beta}, \bar{M}_{\alpha\beta}\} = \int_{-\bar{h}}^{\bar{h}} \bar{S}_{\alpha\beta}\{1, x_3\}\,\mathrm{d}x_3 \tag{21a}$$

$$\bar{N}_{\alpha 3} = \int_{-\bar{h}}^{\bar{h}} \bar{S}_{\alpha 3}\,\mathrm{d}x_3 \tag{21b}$$

The stress resultants and stress couples for the upper facings can be obtained from Eqs. (20) by replacing single primes by double primes, a' by $-a''$ and n' by n''. Herein, n' and n'' denote the number of layers constitutent to the bottom and upper facings, respectively, whereas $(x_3)_k$ and $(x_3)_{k-1}$ denote the distances from the global reference surface (coinciding with that of the core layer) to the upper and bottom interfaces of the kth layer, respectively. These definitions of stress resultants and stress couples are similar to the ones in Refs. 4 and 5.

The associated boundary conditions at the edge $x_n = \text{const}$ ($n = 1, 2$) result as

$$N_{nn} = \underset{\sim}{N}_{nn} \quad \text{or} \quad \xi_n = \underset{\sim}{\xi}_n \tag{22a}$$

$$N_{nt} = \underset{\sim}{N}_{nt} \quad \text{or} \quad \xi_t = \underset{\sim}{\xi}_t \tag{22b}$$

$$L_{nn} = \underset{\sim}{L}_{nn} \quad \text{or} \quad \eta_n = \underset{\sim}{\eta}_n \tag{22c}$$

$$L_{nt} = \underset{\sim}{L}_{nt} \quad \text{or} \quad \eta_t = \underset{\sim}{\eta}_t \tag{22d}$$

$$\hat{H}_{nn} = \underset{\sim}{\hat{H}}_{nn} \quad \text{or} \quad \psi'_n = \underset{\sim}{\psi}'_n \tag{22e}$$

$$\hat{H}_{nt} = \underset{\sim}{\hat{H}}_{nt} \quad \text{or} \quad \psi'_t = \underset{\sim}{\psi}'_t \tag{22f}$$

$$\hat{\hat{H}}_{nn} = \underset{\sim}{\hat{\hat{H}}}_{nn} \quad \text{or} \quad \psi''_n = \underset{\sim}{\psi}''_n \tag{22g}$$

$$\hat{\hat{H}}_{nt} = \underset{\sim}{\hat{\hat{H}}}_{nt} \quad \text{or} \quad \psi''_t = \underset{\sim}{\psi}''_t \tag{22h}$$

$$N_{nt}(v_{3,t} + \mathring{v}_{3,t}) + N_{nn}(v_{3,n} + \mathring{v}_{3,n}) + N_{n3} = \underset{\sim}{N}_{n3} \quad \text{or} \quad v_3 = \underset{\sim}{v}_3 \tag{22i}$$

Here the subscripts n and t are used to designate the normal and tangential in-plane directions to an edge, and hence $n = 1$ when $t = 2$ and vice versa.

Special Cases

A. Discard of Transverse Shear Effects in the Facings

In the case of thin facings or when the constituent materials feature large transverse shear stiffness characteristics, the Love–Kirchhoff hypothesis can be adopted for the facings.

In this case, from the variational principle, Eq. (14), using Eqs. (13a) properly, the equations of equilibrium/motion become

$$\delta\xi_1:\ N_{11,1} + N_{12,2} = 0 \tag{23a}$$

$$\delta\xi_2:\ N_{22,2} + N_{12,1} = 0 \tag{23b}$$

$$\delta\eta_1:\ L_{11,1} + L_{12,2} - \bar{N}_{13} = 0 \tag{23c}$$

$$\delta\eta_2:\ L_{22,2} + L_{12,1} - \bar{N}_{23} = 0 \tag{23d}$$

$$\begin{aligned}\delta v_3:\ & N_{11}(v_{3,11} + \mathring{v}_{3,11} + 1/R_1) + 2N_{12}(v_{3,12} + \mathring{v}_{3,12}) \\ & + N_{22}(v_{3,22} + \mathring{v}_{3,22} + 1/R_2) - C_2(\bar{N}_{11,11} + 2\bar{N}_{12,12} + \bar{N}_{22,22}) \\ & + (M_{11,11} + 2M_{12,12} + M_{22,22}) + (1 + C_1/\bar{h}) \\ & \times (\bar{N}_{13,1} + \bar{N}_{23,2}) + q_3 - m_0\ddot{v}_3 = 0\end{aligned} \tag{23e}$$

Similarily, the associated boundary conditions become

$$N_{nn} = \underset{\sim}{N}_{nn} \quad \text{or} \quad \xi_n = \underset{\sim}{\xi}_n \tag{24a}$$

$$N_{nt} = \underset{\sim}{N}_{nt} \quad \text{or} \quad \xi_t = \underset{\sim}{\xi}_t \tag{24b}$$

$$L_{nn} = \underset{\sim}{L}_{nn} \quad \text{or} \quad \eta_n = \underset{\sim}{\eta}_n \tag{24c}$$

$$L_{nt} = \underset{\sim}{L}_{nt} \quad \text{or} \quad \eta_t = \underset{\sim}{\eta}_t \tag{24d}$$

$$C_2\bar{N}_{nn} - M_{nn} = C_2\underset{\sim}{\bar{N}}_{nn} - \underset{\sim}{M}_{nn} \quad \text{or} \quad v_{3,n} = \underset{\sim}{v}_{3,n} \tag{24e}$$

$$\begin{aligned}& N_{nt}(v_{3,t} + \mathring{v}_{3,t}) + N_{nn}(v_{3,n} + \mathring{v}_{3,n}) + M_{nn,n} \\ & + 2M_{nt,t} - C_2(\bar{N}_{nn,n} + 2\bar{N}_{nt,t}) + (1 + C_1/\bar{h})\bar{N}_{n3} \\ & = -C_2\underset{\sim}{\bar{N}}_{nt,t} + \underset{\sim}{M}_{nt,t} + \underset{\sim}{\bar{N}}_{n3} \quad \text{or} \quad v_3 = \underset{\sim}{v}_3\end{aligned} \tag{24f}$$

Note that, in contrast to the case of sandwich structures whose faces are flexible in transverse shear (when nine boundary conditions have to be prescribed at each edge), in this special case only six boundary conditions have to be prescribed. This implies that, consistent with the number of boundary conditions, in the former case the system of governing equations should be of the 18th order, whereas in the latter one it should be of the 12th order.

Equations (23) and (24) specialized for the case of flat sandwich plates coincide with those derived in Refs. 4 and 5.

In Eqs. (23) and (24), the global stress resultants and stress couples are defined as

$$N_{11} = {}'N_{11} + \bar N_{11} + {}''N_{11} \qquad (1 \rightleftarrows 2) \tag{25a}$$

$$N_{12} = {}'N_{12} + \bar N_{12} + {}''N_{12} \tag{25b}$$

$$L_{11} = \bar h({}'N_{11} - {}''N_{11}) + \bar M_{11} \qquad (1 \rightleftarrows 2) \tag{25c}$$

$$L_{12} = \bar h({}'N_{12} - {}''N_{12}) + \bar M_{12} \tag{25d}$$

$$M_{11} = {}'M_{11} + {}''M_{11} - (C_1/\bar h)\bar M_{11} \qquad (1 \rightleftarrows 2) \tag{25e}$$

$$M_{12} = {}'M_{12} + {}''M_{12} - (C_1/\bar h)\bar M_{12} \tag{25f}$$

where

$$C_1 = \frac{h' + h''}{4} \tag{26a}$$

$$C_2 = \frac{h' - h''}{4} \tag{26b}$$

B. Soft Core Sandwich Shell

In the case of the soft core sandwich structures, $\bar N_{\alpha\beta}$ and $\bar M_{\alpha\beta}$ should be considered zero-valued quantities in the expressions of the global stress resultants and stress couples [Eqs. (25)]. As a result, the proper equations for this case can be obtained in a straightforward manner.

Constitutive Equations

Preparatory to the derivation of constitutive equations for sandwich shells, it should be recalled that within the three-dimensional geometrically nonlinear elasticity theory the constitutive equations are described by linear relationships between the second Piola–Kirchhoff stress and Lagrange strain tensor components.

As a result, for an anisotropic material featuring monoclinic symmetry and including the temperature and moisture effects, the generalized Hooke law can be expressed as

$$\begin{Bmatrix} S_{11} \\ S_{22} \\ S_{12} \end{Bmatrix} = \begin{bmatrix} \hat Q_{11} & \hat Q_{12} & \hat Q_{16} \\ \hat Q_{12} & \hat Q_{22} & \hat Q_{26} \\ \hat Q_{16} & \hat Q_{26} & \hat Q_{66} \end{bmatrix} \begin{Bmatrix} e_{11} \\ e_{22} \\ 2e_{12} \end{Bmatrix} - \begin{Bmatrix} \hat\lambda_{11} \\ \hat\lambda_{22} \\ \hat\lambda_{12} \end{Bmatrix} T - \begin{Bmatrix} \hat\mu_{11} \\ \hat\mu_{22} \\ \hat\mu_{12} \end{Bmatrix} M \tag{27a}$$

$$\begin{Bmatrix} S_{23} \\ S_{13} \end{Bmatrix} = K^2 \begin{bmatrix} Q_{44} & Q_{45} \\ Q_{45} & Q_{55} \end{bmatrix} \begin{Bmatrix} 2e_{23} \\ 2e_{13} \end{Bmatrix} \tag{27b}$$

(see Ref. 14). In these equations, S_{ij} denotes the second Piola–Kirchhoff stress tensor, $\hat Q_{ij}[\equiv Q_{ij} - (Q_{i3}Q_{j3}/Q_{33})]$ are the reduced elastic moduli, $\hat\lambda_{ij}[\equiv \lambda_{ij} - (Q_{I3}/Q_{33})\lambda_{33})]$ and $\hat\mu_{ij}[\equiv \mu_{ij} - (Q_{I3}/Q_{33})\mu_{33})]$ denote the reduced thermal expansion and moisture swelling coefficients, respectively, where $T[\equiv T(x_\alpha, x_3)]$ and $M[\equiv M(x_\alpha, x_3)]$ denote the excess of temperature and moisture with respect to free stress temperature and moisture T_r and M_r, respectively. Herein the index I takes the values 1, 2, or 6 when the pair of indices ij assumes the values 11, 22, or 12, respectively.

Because the anisotropic material featuring a monoclinic symmetry can simulate an orthotropic material whose axes of orthotropy are rotated with respect to the geometrical axes of the structure, the elastic, thermal, and moisture moduli, $\hat Q_{ij}$, $\hat\lambda_{ij}$, and $\hat\mu_{ij}$, respectively, can be expressed in terms of the associated elastic, thermal expansion, and moisture swelling moduli in the on-axis configuration and the angles by which the principal material axes are rotated with respect to the geometrical ones, i.e., the ply angles. These relationships are not displayed here.

Employment in Eqs. (20) of Eqs. (27) results in the constitutive equations for the bottom facings. These are expressed in compact form as

$$\begin{aligned} {}'N_{11} = {} & A'_{11}\varepsilon'_{11} + A'_{12}\varepsilon'_{22} + A'_{16}\gamma'_{12} + E'_{11}\kappa'_{11} \\ & + E'_{12}\kappa'_{22} + E'_{16}\kappa'_{12} - {}'N^T_{11} - {}'N^m_{11} \qquad (1 \rightleftarrows 2) \end{aligned} \tag{28a}$$

$$\begin{aligned} {}'N_{12} = {} & A'_{16}\varepsilon'_{11} + A'_{26}\varepsilon'_{22} + A'_{66}\gamma'_{12} + E'_{16}\kappa'_{11} \\ & + E'_{26}\kappa'_{22} + E'_{66}\kappa'_{12} - {}'N^T_{12} - {}'N^m_{12} \end{aligned} \tag{28b}$$

$${}'N_{23} = {}'K^2[{}'A_{44}\gamma'_{23} + {}'A_{45}\gamma'_{13}] \tag{28c}$$

$${}'N_{13} = {}'K^2[{}'A_{45}\gamma'_{23} + {}'A_{55}\gamma'_{13}] \tag{28d}$$

$$\begin{aligned} {}'M_{11} = {} & E'_{11}\varepsilon'_{11} + E'_{12}\varepsilon'_{22} + E'_{16}\gamma'_{12} + F'_{11}\kappa'_{11} \\ & + F'_{12}\kappa'_{22} + F'_{16}\kappa'_{12} - {}'M^T_{11} - {}'M^m_{11} \qquad (1 \rightleftarrows 2) \end{aligned} \tag{28e}$$

$$\begin{aligned} {}'M_{12} = {} & E'_{16}\varepsilon'_{11} + E'_{26}\varepsilon'_{22} + E'_{66}\gamma'_{12} + F'_{16}\kappa'_{11} \\ & + F'_{26}\kappa'_{22} + F'_{66}\kappa'_{12} - {}'M^T_{12} - {}'M^m_{12} \end{aligned} \tag{28f}$$

The stiffness quantities appearing in Eqs. (28) are defined as

$$\{A'_{\omega\rho}, B'_{\omega\rho}, D'_{\omega\rho}\} = \sum^{n'} \int_{(x_3)_{k-1}}^{(x_3)_k} (\hat Q'_{\omega\rho})_{(k)}(1, x_3, x_3^2)\,\mathrm{d}x_3 \qquad (\omega, \rho = 1, 2, 6) \tag{29a}$$

$$A'_{IJ} = {}'K^2 \sum^{n'} \int_{(x_3)_{k-1}}^{(x_3)_k} (Q'_{IJ})\,\mathrm{d}x_3 \qquad (I, J = 4, 5) \tag{29b}$$

$${}'N^T_{\alpha\beta} = \sum^{n'} \int_{(x_3)_{k-1}}^{(x_3)_k} ({}'\hat\lambda_{\alpha\beta})_k T\,\mathrm{d}x_3 \tag{29c}$$

$${}'N^m_{\alpha\beta} = \sum^{n'} \int_{(x_3)_{k-1}}^{(x_3)_k} ({}'\hat\mu_{\alpha\beta})_k M\,\mathrm{d}x_3 \tag{29d}$$

$${}'M^T_{\alpha\beta} = \sum^{n'} \int_{(x_3)_{k-1}}^{(x_3)_k} (x_3 - a')({}'\hat\lambda_{\alpha\beta})_k T\,\mathrm{d}x_3 \tag{29e}$$

$${}'M^m_{\alpha\beta} = \sum^{n'} \int_{(x_3)_{k-1}}^{(x_3)_k} (x_3 - a')({}'\hat\mu_{\alpha\beta})_k M\,\mathrm{d}x_3 \qquad (\alpha, \beta = 1, 2) \tag{29f}$$

whereas

$$E'_{\omega\rho} = B'_{\omega\rho} - a'A'_{\omega\rho} \tag{30a}$$

$$F'_{\omega\rho} = D'_{\omega\rho} - 2a'B'_{\omega\rho} + a'^2 A'_{\omega\rho} \tag{30b}$$

The expression of stress resultants and stress couples for the upper facings can be formally obtained from Eqs. (28) by replacing the single prime by double primes. In the case when bottom and upper facings feature full symmetry about their own midsurfaces, $E'_{\omega\rho}$ and $E''_{\omega\rho} \equiv 0$.

For the core layer considered as an orthotropic body (the axes of orthotropy coinciding with the geometrical axes), the constitutive equations are

$$\bar N_{11} = 2\bar h[\bar Q_{11}\bar\varepsilon_{11} + \bar Q_{12}\bar\varepsilon_{22}] - \bar N^T_{11} - \bar N^m_{11} \qquad (1 \rightleftarrows 2) \tag{31a}$$

$$\bar N_{12} = 2\bar h\,\bar Q_{66}\bar\gamma_{12} \tag{31b}$$

$$\bar N_{13} = 2\bar h\,\bar K^2\bar Q_{55}\bar\gamma_{13} \qquad (1 \rightleftarrows 2) \tag{31c}$$

$$\bar M_{11} = \tfrac{2}{3}\bar h^3[\bar Q_{11}\bar\kappa_{11} + \bar Q_{12}\bar\kappa_{22}] - \bar M^T_{11} - \bar M^m_{11} \qquad (1 \rightleftarrows 2) \tag{31d}$$

$$\bar M_{12} = \tfrac{2}{3}\bar h^3\bar Q_{66}\bar\kappa_{12} \tag{31e}$$

where

$$(\bar N^T_{\alpha\beta}, \bar M^T_{\alpha\beta}) = \int_{-\bar h}^{\bar h} (1, x_3)\bar\lambda_{\alpha\beta}T\,\mathrm{d}x_3 \qquad (\alpha, \beta = 1, 2) \tag{32a}$$

$$(\bar N^m_{\alpha\beta}, \bar M^m_{\alpha\beta}) = \int_{-\bar h}^{\bar h} (1, x_3)\bar\mu_{\alpha\beta}M\,\mathrm{d}x_3 \tag{32b}$$

In Eqs. (28), (29), and (31), ${}'K^2$ and $\bar K^2$ denote transverse shear correction factors associated with facings and core, respectively.

Governing Equations

Preliminaries

One possible and most straightforward representation of the governing equations in the theory of shells in general and of sandwich-type structures in particular is that in terms of displacement quantities. However, as the recent results in the area reveal, the formulation of shear deformable shallow shell theory in terms of Airy's potential function, the transversal deflection, and a transverse shear potential function presents many advantages, especially in the study of their buckling and postbuckling response, e.g., Refs. 15–18.

For sandwich structures, however, only in special cases this type of formulation can exactly be applied. One notable case for which this representation can be carried out is that of weak core sandwich shells/plates with symmetrically distributed faces about both the global and local midsurfaces. In the forthcoming developments this representation is applied to this type of sandwich shells/plates.

Weak-Core Sandwich-Type Shells/Plates

To get a better understanding of the influence played by a number of effects on buckling and postbuckling responses of sandwich shells/plates with weak cores, this formulation will be restricted to the case of 1) thin face sheets, thus enabling one to discard transverse shear effects in the facings, 2) restriction to the static case and the absence of temperature and moisture effects, 3) consideration of circular cylindrical panels and of their flat counterparts, and 4) consideration of symmetric sandwich constructions, implying that the upper and bottom face sheets feature the same thickness and identical stacking sequence and are both symmetrically laminated about their respective midsurfaces.

Under such conditions, the exact fulfillment of Eqs. (23a) and (23b) results in the representation

$$N_{11} = \phi_{,22} \tag{33a}$$

$$N_{22} = \phi_{,11} \tag{33b}$$

$$N_{12} = -\phi_{,12} \tag{33c}$$

where $\phi \equiv \phi(x_\alpha)$ is Airy's potential function. With the help of Eqs. (33) and by virtue of assumption 4) implying

$$A'_{\alpha\beta} = A''_{\alpha\beta} \equiv A_{\alpha\beta} \tag{34a}$$

$$F'_{\alpha\beta} = F''_{\alpha\beta} \equiv F_{\alpha\beta} \tag{34b}$$

$$E'_{\alpha\beta} = E''_{\alpha\beta} = 0 \tag{34c}$$

$$a' = a'' \equiv a, \qquad h' = h'' \equiv h, \qquad C_2 = 0 \tag{34d}$$

the remaining equations of equilibrium (23c–23e) expressed in terms of Airy's potential function and the displacement quantities become

$$\begin{aligned} &A_{11}\eta_{1,11} + A_{16}\eta_{2,11} + A_{66}\eta_{1,22} + (A_{12} + A_{66})\eta_{2,12} + 2A_{16}\eta_{1,12} \\ &\quad + A_{26}\eta_{2,22} - (2\bar{K}^2\bar{G}_{13}/\bar{h})(\eta_1 + av_{3,1}) = 0 \qquad (1 \rightleftarrows 2) \end{aligned} \tag{35a}$$

$$\begin{aligned} &\phi_{,22}(v_{3,11} + \mathring{v}_{3,11} + 1/R_1) + \phi_{,11}(v_{3,22} + \mathring{v}_{3,22} + 1/R_2) \\ &\quad - 2\phi_{,12}(v_{3,12} + \mathring{v}_{3,12}) - F_{11}v_{3,1111} - F_{22}v_{3,2222} - 4F_{16}v_{3,1112} \\ &\quad - 4F_{26}v_{3,1222} - 2(F_{12} + 2F_{66})v_{3,1122} + (2\bar{K}^2 a/\bar{h}) \\ &\quad \times \{\bar{G}_{13}(\eta_{1,1} + av_{3,11}) + \bar{G}_{23}(\eta_{2,2} + av_{3,22})\} + q_3 = 0 \end{aligned} \tag{35b}$$

Recalling that the equations of equilibrium (23a) and (23b) are identically fulfilled via the use of the stress potential function, to ensure single valued displacements, the compatibility equation for the membrane strains has to be satisfied as well.

For the problem at hand the compatibility equation is

$$\begin{aligned} &\varepsilon_{11,22} + \varepsilon_{22,11} - \gamma_{12,12} + (2/R_1)v_{3,22} + (2/R_2)v_{3,11} - 2v_{3,12}^2 \\ &\quad + 2v_{3,11}v_{3,22} + 2\mathring{v}_{3,11}v_{3,22} - 4v_{3,12}\mathring{v}_{3,12} + 2v_{3,11}\mathring{v}_{3,22} = 0 \end{aligned} \tag{36}$$

where

$$\varepsilon_{11} = {}'\varepsilon_{11} + {}''\varepsilon_{11}, \qquad \varepsilon_{22} = {}'\varepsilon_{22} + {}''\varepsilon_{22}, \qquad \gamma_{12} = {}'\gamma_{12} + {}''\gamma_{12}$$

To express this equation in terms of the basic unknown functions, a partial inversion of constitutive equations (28a) has to be carried out. With the use of these equations, Eq. (36) reduces to

$$\begin{aligned} &A^*_{22}\phi_{,1111} + A^*_{11}\phi_{,2222} - 2A^*_{16}\phi_{,1222} - 2A^*_{26}\phi_{,2111} \\ &\quad + (A^*_{66} + 2A^*_{12})\phi_{,1122} + (2/R_1)v_{3,22} + (2/R_2)v_{3,11} - 2v_{3,12}^2 \\ &\quad + 2v_{3,11}v_{3,22} + 2\mathring{v}_{3,11}v_{3,22} + 2v_{3,11}\mathring{v}_{3,22} - 4v_{3,12}\mathring{v}_{3,12} = 0 \end{aligned} \tag{37}$$

Equation (37) is included as a primary field equation of the nonlinear boundary value problem along with Eqs. (35). As a result, the equations for the problem at hand reduce to four partial differential equations expressed in terms of the functions η_1, η_2, v_3, and ϕ.

In connection with the stiffness quantities ${}'A^*_{\omega\rho} = {}''A^*_{\omega\rho} \equiv A^*_{\omega\rho}$, ($\omega, \rho = 1, 2, 6$) appearing in Eq. (37), ${}'A^*_{\omega\rho}$ and ${}''A^*_{\omega\rho}$ represent the inverted counterparts of ${}'A_{\omega\rho}$ and ${}''A_{\omega\rho}$, respectively.

Postbuckling Solution

The governing equations of shallow circular cylindrical sandwich panels with weak cores as expressed by Eqs. (35) and (37) represent an extension of those known under the name of von Kármán–Marguerre–Mushtary, which are pertinent to the classical nonlinear shallow shell theory (e.g., Ref. 5), of their shear deformable counterpart (e.g., Refs. 15–18), as well as of the governing equations of flat sandwich panels as derived in Refs. 4 and 5.

To assess the influence played by a number of nonclassical effects, in addition to the assumptions stated earlier, the case of sandwich constructions featuring cross-ply laminated facings is considered, implying $A_{16} = A_{26} = 0$ and $F_{16} = F_{26} = 0$.

The analysis will be confined to simply supported boundary conditions. Because for geometrically nonlinear problems the bending and stretching problems are coupled, in addition to the bending boundary conditions, the ones associated with the tangential boundary conditions also have to be fulfilled. The formulation of the latter ones gives rise to two tangential types of boundary conditions, referred to herein as movable and immovable edge conditions. These correspond to the case when the motion of the unloaded edges is either unrestrained or completely restrained, respectively, in the plane tangent to the structure's midsurface, normal to the respective edge. As a result we have the following cases. Case I: Edges $x_n =$ const ($n = 1, 2$) are compressed and freely movable. In this case, along these edges the following conditions have to be fulfilled:

$$N_{nn} = -\underset{\sim}{N}_{nn} \tag{38a}$$

$$N_{nt} = 0 \tag{38b}$$

$$\eta_n = 0 \tag{38c}$$

$$\eta_t = 0 \tag{38d}$$

$$M_{nn} = 0 \tag{38e}$$

$$v_3 = 0 \tag{38f}$$

Case II: Edges $x_n =$ const are unloaded and immovable. In this case,

$$\xi_n = 0 \tag{39a}$$

$$N_{nt} = 0 \tag{39b}$$

$$\eta_n = 0 \tag{39c}$$

$$\eta_t = 0 \tag{39d}$$

$$M_{nn} = 0 \tag{39e}$$

$$v_3 = 0 \tag{39f}$$

As earlier, n and t designate the normal and tangential in-plane directions to an edge.

The condition expressing the immovability conditions $\xi_n = 0$ on $x_n =$ const is fulfilled in an average sense as

$$\int_0^{L_1}\int_0^{L_2} \frac{\partial \xi_n}{\partial x_n}\,\mathrm{d}x_n\,\mathrm{d}x_t = 0$$

This condition, in conjunction with Eq. (A1) from the Appendix, provides the fictitious edge load N_{nn}, rendering the edges $x_n =$ const immovable.

The expression of transverse deflection satisfying the simply supported boundary conditions is

$$v_3(x_1, x_2) = w_{mn} \sin \lambda_m x_1 \sin \mu_n x_2$$

$$(m = 1, 2, \ldots, M; \qquad n = 1, 2, \ldots, N) \qquad (40a)$$

where $\lambda_m = m\pi/L_1$, $\mu_n = n\pi/L_2$, and w_{mn} are the modal amplitudes, whereas L_1 and L_2 are the panel side edges. Following the results of Ref. 19, the representation of initial geometric imperfections resulting, for the problem at hand, in the most critical postbuckling conditions is

$$\mathring{v}_3(x_1, x_2) = \mathring{w}_{mn} \sin \lambda_m x_1 \sin \mu_n x_2 \qquad (40b)$$

where $\mathring{w}_{mn}$ are the model amplitudes of the initial geometric imperfection shape. Moreover, the stress function ϕ is expressed as

$$\phi(x_\omega) = \phi_1(x_\omega) - \tfrac{1}{2}\left(N_{11}x_2^2 + N_{22}x_1^2 - 2N_{12}x_1x_2\right) \qquad (41)$$

(see Refs. 5 and 20), where, as shown (see Refs. 16–18 and 20), N_{11}, N_{22}, and N_{12} represent the average compressive and shear edge loads whereas ϕ_1 is a particular solution of Eq. (37). Replacing Eq. (40) into the compatibility equation (37) and solving the resulting nonhomogeneous partial differentiation equation yield the expression of ϕ_1 as

$$\phi_1(x_\alpha) = A_1 \cos 2\lambda_m x_1 + A_2 \cos 2\mu_n x_2 + A_3 \sin \lambda_m x_1 \sin \mu_n x_2 \qquad (42)$$

Similarly, the two coupled equations, namely, Eq. (35a) and its counterpart obtained by applying the change ($1 \leftrightarrows 2$), can be solved to get

$$\eta_1(x_\omega) = B_1 \cos \lambda_m x_1 \sin \mu_n x_2 \qquad (43a)$$

$$\eta_2(x_\omega) = C_1 \sin \lambda_m x_1 \cos \mu_n x_2 \qquad (43b)$$

Furthermore, the use of Eqs. (33) in conjunction with the expression of $N_{\alpha\beta}$ in terms of the displacement quantities and of Eqs. (42) and (43) enables one to obtain the displacements $\xi_1(x_\omega)$ and $\xi_2(x_\omega)$. Due to their intricacy, these expressions of those coefficients B_1 and C_1 in Eqs. (43) and of the coefficients A_i ($i = 1, 2, 3$) in Eqs. (42) are not recorded here.

One of the methods yielding the postbuckling equations in terms of the modal amplitudes w_{mn} is to solve Eq. (35b) in the Galerkin sense (e.g., Refs. 18 and 20). However, a more inclusive method, enabling one, among others, to compensate the nonfulfillment of certain boundary conditions, such as of static ones, rests on the use of the extended Galerkin method (e.g., Ref. 21). To this end, replacing the expressions of ϕ, v_3, $\mathring{v}_3$, η_1, η_2, ξ_1, and ξ_2 into the energy functional, Eq. (14), and carrying out the indicated integrations result in the following nonlinear algebraic equation expressed in terms of the modal amplitudes $\delta_{mn} (\equiv w_{mn}/H)$ as

$$P_1[\delta_{mn}, \mathring{\delta}_{mn}, \mathcal{N}_1, \mathcal{N}_2] + P_2[\delta_{mn}^2, \mathring{\delta}_{mn}] + P_3[\delta_{mn}^3, \delta_{mn}^2, \mathring{\delta}_{mn}, \delta_{mn}]$$
$$+ P_{mn}[(\mathcal{N}_1/R_2) + (\mathcal{N}_2/R_1)] = 0$$
$$(m = 1, \ldots, M; \qquad n = 1, \ldots, N) \qquad (44)$$

In this equation P_1, P_2, and P_3 are linear, quadratic, and cubic polynomials of the unknown modal amplitudes; P_{mn} are constants that depend on the material and geometric properties of the shell; $\mathcal{N}_1$ and $\mathcal{N}_2$ are normalized forms of normal edge loads to be defined later; and $\mathring{\delta}_{mn} (\equiv \mathring{w}_{mn}/H)$ denotes the modal imperfection amplitudes.

The equilibrium configurations for a given flat or curved panel are determined by solving the nonlinear algebraic equation (44) via Newton's method. As a byproduct, the values of $\mathcal{N}_1$ and $\mathcal{N}_2$ fulfilling the linearized counterpart of Eqs. (44) corresponding to $\delta_{mn} \neq 0$ can be obtained. These correspond to the buckling bifurcation solution. In the following, a number of numerical illustrations related to the buckling and postbuckling behavior are displayed.

Results and Discussion

A. Comparisons with Available Experimental Data

Results on the buckling response predicted by the present structural model are compared with their experimental counterparts[22] and displayed in Tables 1 and 2.

In Table 1 a three-layer symmetric flat sandwich panel with isotropic facings (of Dura-Aluminum, $\nu = 0.3$ and $E = 6.96 \times 10^5$ kg/cm^2) and a transversely isotropic weak core (of penoplast) uniaxially compressed is considered.

The results associated with the tables show a reasonable agreement. Note that the theoretical results reveal, in general, slight overpredictions of the experimental ones. Consideration of unavoidable

Table 1 Comparisons of theoretical and experimental buckling predictions for a flat sandwich panel with transversely isotropic core (simply supported edge conditions)

						$N_{11}L_2 \times 10^3$ kg		
Case	L_1, cm	L_2, cm	h, cm	$\bar{h}$, cm	$\bar{G}$, kg/cm^2	Theory	Exp.	Error, %
1	60	40	0.05	0.425	99.4	3.79	3.60	+5.28
2	60	40	0.10	0.650	149.6	9.03	8.25	+9.45
3	40	60	0.10	0.700	117.1	11.30	12.30	−8.13
4	40	60	0.10	1.400	96.5	17.40	16.00	+8.75
5	80	60	0.05	0.450	73.5	4.21	4.00	+5.25
6	80	60	0.05	0.450	74.1	4.24	4.10	+3.41

Table 2 Comparisons of theoretical and experimental buckling predictions for a sandwich flat panel with orthotropic core and isotropic faces (simply supported edge conditions)

							$N_{11}L_2 \times 10^3$ kg		
Case	L_1, cm	L_2, cm	h, cm	$\bar{h}$, cm	$\bar{G}_{13}$, kg/cm^2	$\bar{G}_{23}$, kg/cm^2	Theory	Exp.	Error, %
1	60	40	0.05	0.45	140.4	100.8	5.29	5.85	−9.57
2	60	40	0.25	1.25	390.0	103.0	47.22	46.57	+1.11
3	60	40	0.25	1.15	337.0	97.0	38.20	36.50	+4.66
4	80	60	0.10	0.95	138.1	78.6	17.34	15.25	+13.7

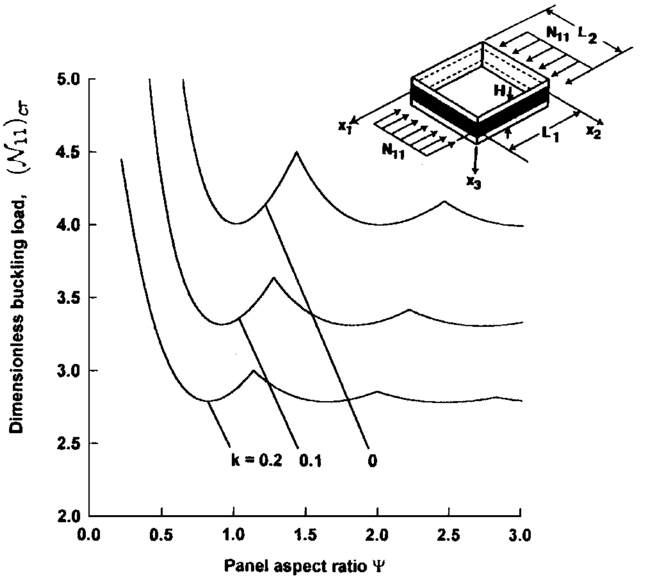

Fig. 1 Variation of dimensionless buckling coefficient $(\mathcal{N}_1)_{cr}$ vs panel aspect ratio ψ. Isotropic faces ($\nu_f = 0.3$ and $\eta = 0.1$) and transversely isotropic core ($k = 0$, 0.1, and 0.2). In the inset, a sandwich flat panel is depicted.

initial geometric imperfections, which probably were present in the tested model, would eliminate this disparity of results.

B. Buckling of Flat and Curved Sandwich Panels

The results pertinent to the buckling problem concern rectangular ($L_1 \times L_2$) flat and circular cylindrical ($R_1 = \infty$, $R_2 \equiv R$) sandwich panels simply supported on the whole contour, the material of the core exhibiting transversely isotropic or orthotropic properties. The results are plotted in the plane $[(\mathcal{N}_{11})_{cr}, \psi)]$. The term $(\mathcal{N}_{11})_{cr}$ denotes the dimensionless uniaxial buckling load, $\psi(\equiv L_1/L_2)$ defines the aspect ratio of the panel, and $(\mathcal{N}_{11}, \mathcal{N}_{22})[\equiv (\tilde{\mathcal{N}}_{11}, \tilde{\mathcal{N}}_{22}), rn^2/(\mu_n^2 F_{22})]$ denotes the dimensionless compressive edge loads. The influence of a number of parameters on the buckling behavior is highlighted in Figs. 1 and 2.

Two such parameters, k_1 and k, defined as $k_1[\equiv \pi^2 Q_{22} h \bar{h}/(L_2^2 K^2 G_{13})]$ for orthotropic faces and orthotropic core and $k[\equiv \pi^2 B \bar{h}/(L_2^2 K^2 G)]$ for isotropic faces and transversely isotropic core, constitute measures of transverse shear flexibility of the overall structure; $\alpha^2\{\equiv L_2^4(1 - \nu^2)/[\pi^4 R^2(\bar{h} + h/2)^2]\}$ is a measure of the curvature of the circular cylindrical panel, and $\eta[\equiv (h/(2\bar{h} + h)]$ defines the thickness ratio.

In the context of the theory of sandwich structures with membrane faces, implying $\eta \rightarrow 0$, the flexural stiffness characteristics of faces are considered zero-valued quantities, whereas the stretching stiffnesses are considered to be finite valued quantities.

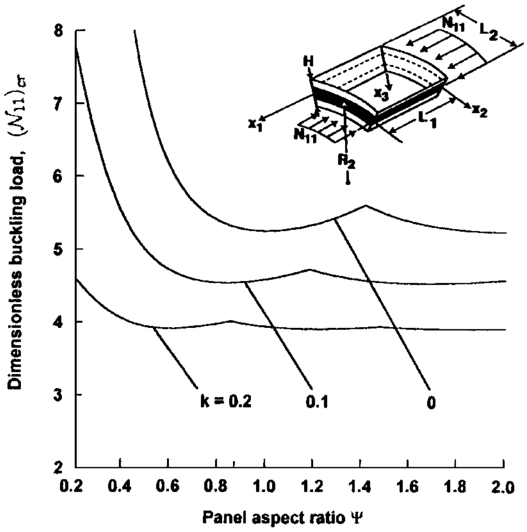

Fig. 2 Variation of dimensionless buckling coefficient $(\mathcal{N}_{11})_{cr}$ vs panel aspect ratio ψ. Circular cylindrical panel ($\alpha^2 = 2.5$) with nonmembrane faces ($\eta = 0.1$). Isotropic faces and transversely isotropic core. In the inset, a sandwich circular cylindrical panel is depicted.

Figure 1 displays the buckling response of flat sandwich panels for various values of k of practical significance, in the context of the nonmembrane concept for the facings. The results of this graph, compared with the ones, not displayed here, obtained when the membrane concept for the facings is adopted, reveal that, in contrast to the former case, in the latter one the buckling load is slightly underestimated. The strong influence played by transverse shear flexibility of the core also becomes apparent, in the sense that, with the increase of transverse shear stiffness of the core [implying the decrease of the parameter k, (k_1)], the buckling load increases.

Figure 2 presents the variation of the buckling loads of sandwich circular cylindrical panels with transversely isotropic core, as a function of the aspect ratio. The results not displayed here reveal that the increase of the shell curvature results in an increase of the buckling load.

In the case of circular cylindrical sandwich panels with orthotropic core, the results not displayed here reveal that the buckling loads are larger than in the case of the transversely isotropic core counterpart.

C. Postbuckling of Flat and Curved Panels

The postbuckling behavior was numerically illustrated for the following cases: 1) flat panels with isotropic facings and transversely isotropic core, 2) flat panels with orthotropic core and orthotropic faces, 3) circular cylindrical panels with isotropic faces and transversely isotropic core, and 4) circular cylindrical panels with orthotropic faces and orthotropic core.

Case 1 concerns simply supported panels whose edges are freely movable in the directions normal to the edges in the plane parallel to the midplane. Figures 3a and 3b display the postbuckling behavior of geometrically perfect/imperfect flat panels in the plane $(\mathcal{N}_{11}, \delta + \delta_0)$ and $(\mathcal{N}_{11}, \Delta_1)$, respectively. Herein $\delta(\equiv w_{11}/H)$ and $\delta_0(\equiv \mathring{w}_{11}/H)$ define the dimensionless deflection and initial geometric imperfection amplitudes in the first mode, whereas

$$\Delta_1\left[\equiv -(L_1 L_2)^{-1}\int_0^{L_1}\int_0^{L_2} \xi_{1,1}\, dx_1\, dx_2\right]$$

defines the end-shortening in the x_1 direction. The results reveal that the decrease of E_f/G_c (implying the increase of the core transverse shear modulus) results in the increase of the load-carrying capacity of the panel. At the same time, as clearly appears, flat panels feature imperfection insensitivity. Herein and in the following illustrations, in contrast to the previous conventions, the quantities affiliated with the core and faces are associated with the index c and f, respectively.

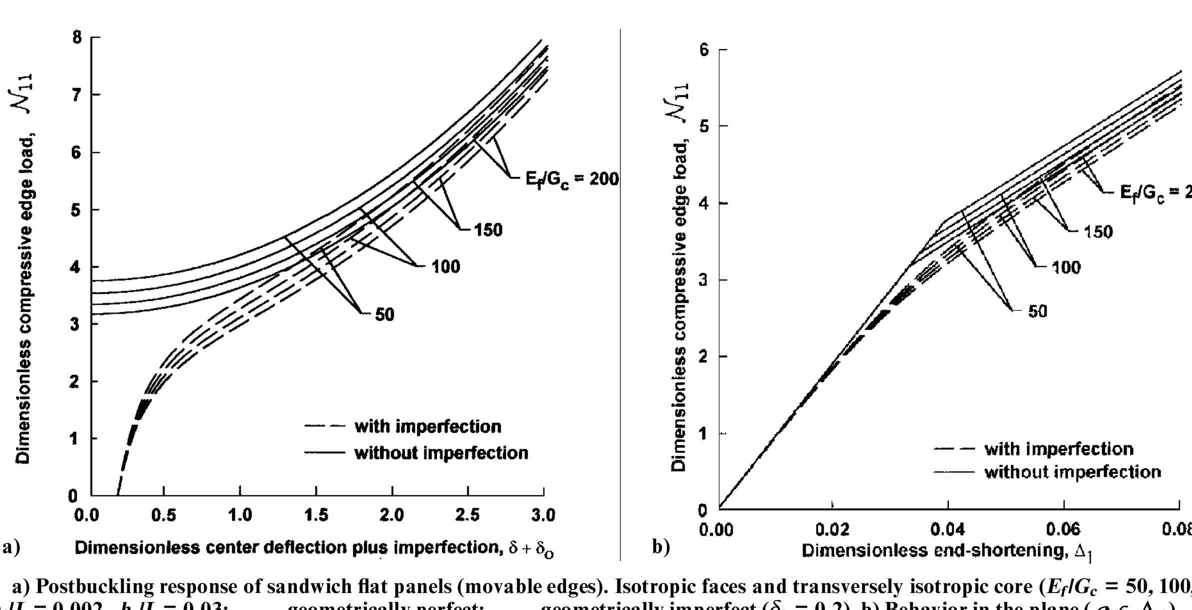

Fig. 3 a) Postbuckling response of sandwich flat panels (movable edges). Isotropic faces and transversely isotropic core (E_f/G_c = 50, 100, 150, and 200; $h_f/L = 0.002$, $h_c/L = 0.03$; ——, geometrically perfect; – – –, geometrically imperfect ($\delta_0 = 0.2$). b) Behavior in the plane $(\mathcal{N}_{11}, \Delta_1)$.

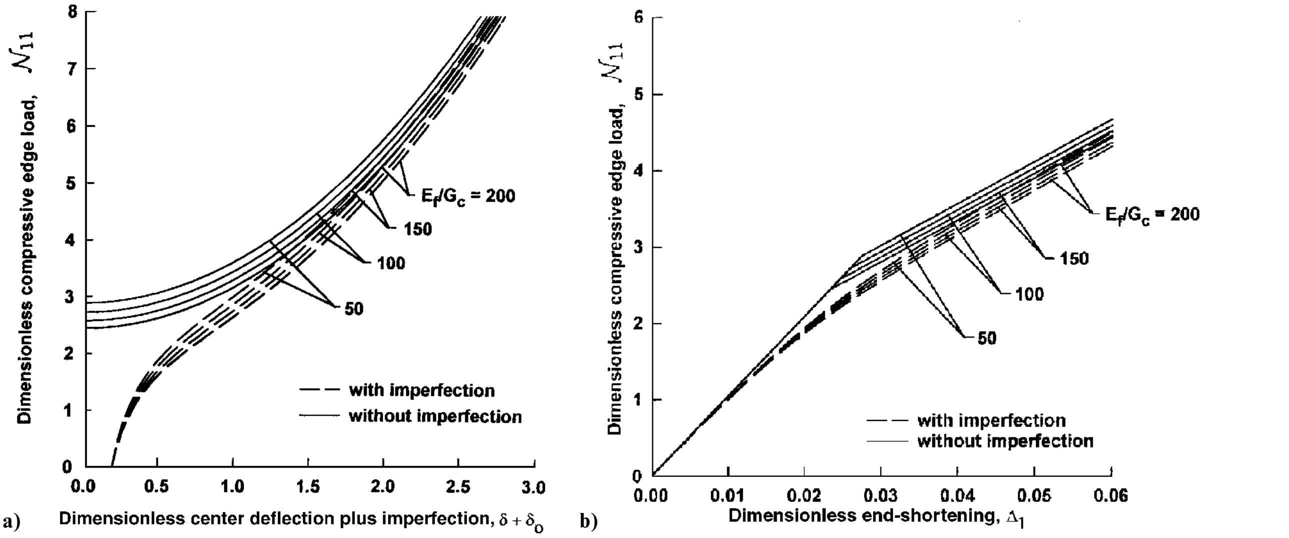

Fig. 4 Counterpart of Fig. 5 for the case of immovable unloaded edges (x_2 = 0, ℓ_2).

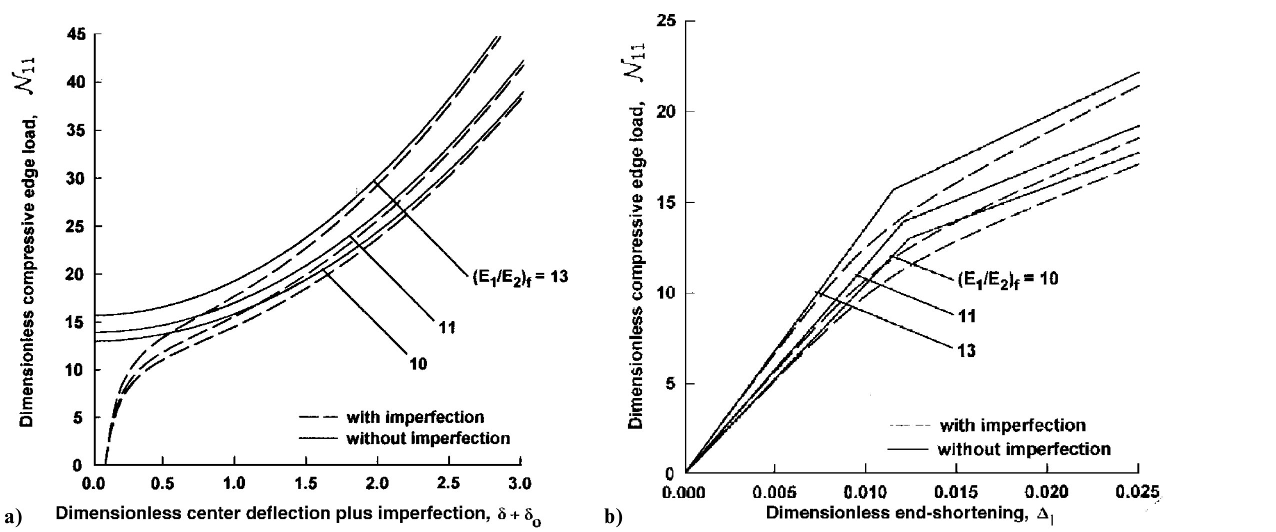

Fig. 5 a) Postbuckling response of sandwich flat panels (movable edges) for three values of the orthotropicity ratio E_1/E_2 of the faces. Orthotropic faces $(G_{12}/E_2)_f$ = 0.6, $(\nu_{21})_f$ = 0.02, and orthotropic core $(E_2)_f/(G_{13})_c$ = 10, $(G_{13}/G_{23})_c$ = 2.5, h_f/L = 0.002, and h_c/L = 0.03; ——, geometrically perfect; – – –, geometrically imperfect (δ_0 = 0.1). b) Behavior in the plane ($\mathcal{N}_{11}$, Δ_1).

Figure 4 represents the counterpart of Fig. 3 for the case of immovable unloaded edges ($x_2 = 0$, L_2). The results reveal that in this case the buckling bifurcation is lower than the one associated with the panel counterpart featuring movable edges. However, in the deep postbuckling range, an enhanced load-carrying capacity and less sensitivity to the variation of E_f/G_c as compared with those featured by the movable edge panels are experienced.

In this case the results show also that in the postbuckling range the load-carrying capacity of the panel becomes less sensitive to the variation of E_f/G_c as compared with the case of the panel featuring movable edges.

For case 2, in Fig. 5 the postbuckling of panels featuring movable edges is considered. Herein, the faces and the core are considered to be orthotropic. In addition to the previously obtained results, it becomes evident that the orthotropicity ratio E_1/E_2 of the facings plays an important role toward enhancing the load-carrying capacity. In addition, the ($\mathcal{N}_{11}$, Δ_1) plot reveals that the increase of the ratio E_1/E_2 tends to prevent the decay of bending stiffness in the postbuckling range.

For case 3, Figs. 6 and 7 depict the postbuckling of uniaxially compressed circular cylindrical panels of square ($L \times L$) projection on a plane. As expected, the results reveal that the load-carrying capacity of the panel increases with the increase of the curvature ratio L/R_2 and with the increase of transverse shear stiffness of the core, i.e., decrease of the ratio E_f/G_c. Moreover, the results emerging from these plots reveal a trend that is not common in the case of the standard laminated curved shells (e.g., Refs. 17 and 18), namely, almost the total absence of the snap-through buckling and of the fact that the load-carrying capacity of the panel is no longer sensitive to initial geometric imperfections. The similarity in this case between the postbuckling response of a plate and shell is noteworthy. This new trend is due to the larger total thickness and, consequently, of the much larger bending stiffness featured by sandwich panels as compared with that of standard laminated constructions.

Finally, results not displayed here obtained for uniaxially compressed circular cylindrical panels featuring orthotropic case and face sheets restate the already mentioned trends related with the influence of orthotropy and curvature on the postbuckling response.

Other results involving buckling and postbuckling, not displayed here, also deserve to be mentioned. For sandwich panels of small curvature ratios L/R_2, the minimum buckling load and the least load-carrying capacity of a circular cylindrical panel characterized by $L_1 = L_2 \equiv L$ occurs at $m = 1, n = 1$. However, with the increase of L/R_2, the minimum buckling load can occur at values of $m(\equiv \bar{m}) \neq 1$. Even so, the results reveal that in the postbuckling range, with the increase of the deflection amplitude $\delta + \delta_0$, the minimum load-carrying capacity is given in succession by postbuckling paths corresponding to $\bar{m}$, $\bar{m} - 1, \ldots, 1, m = 1$ being the mode number providing the minimum load-carrying capacity in the deep postbuckling range.

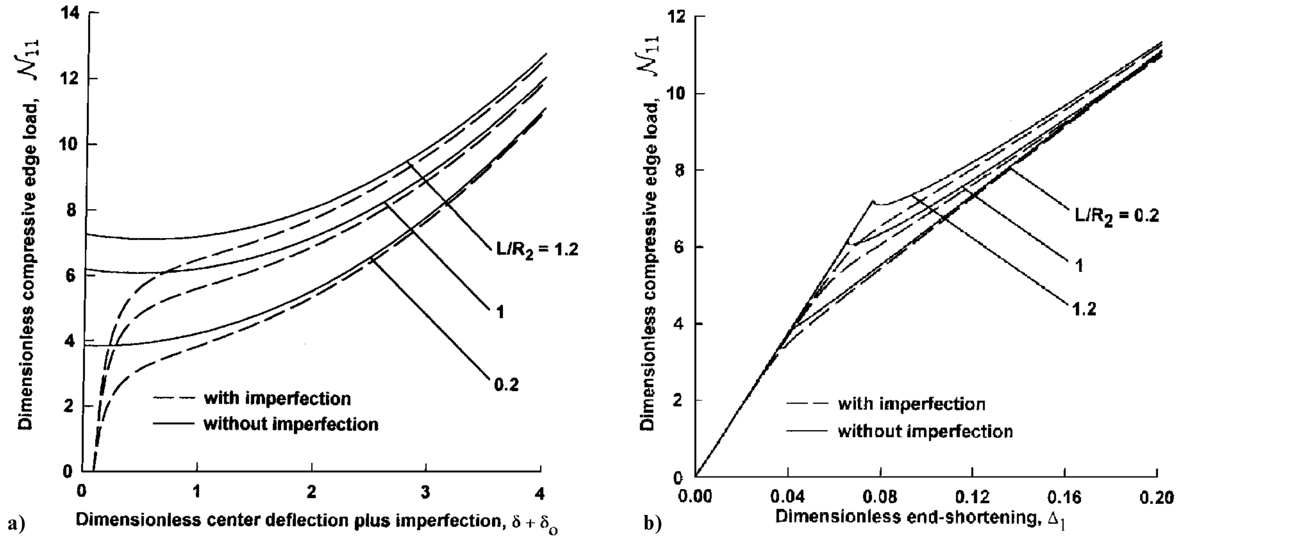

Fig. 6 a) Postbuckling response of circular cylindrical sandwich panels (movable edges) for three values of the curvature ratio (L/R = 1.2, 1, and 0.2). Isotropic faces (ν_f = 0.3) and transversely isotropic core (E_f/G_c = 50), h_f/L = 0.002, h_c/L = 0.03. b) Behavior in the plane ($\mathcal{N}_{11}$, Δ_1).

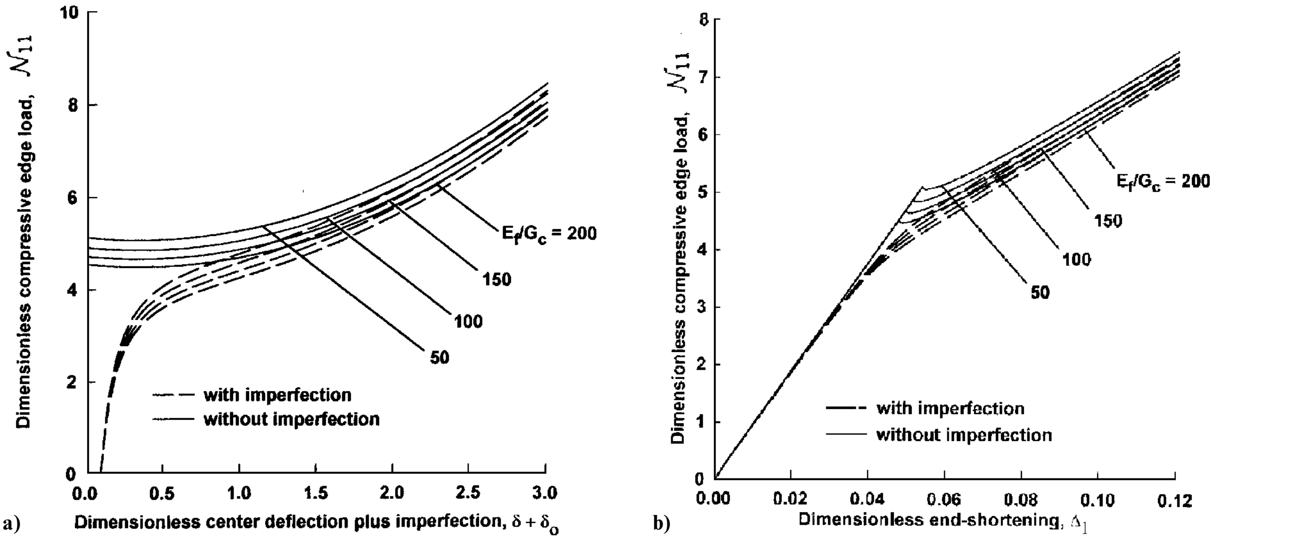

Fig. 7 a) Postbuckling response of circular cylindrical sandwich panels (movable edges) (L/R = 0.76) for four values of the ratio E_f/G_c (50, 100, 150, and 200), h_f/L = 0.002, h_c/L = 0.03, isotropic faces (ν_f = 0.3), and transversely isotropic core. b) Behavior in the plane ($\mathcal{N}_{11}$, Δ_1).

Conclusions

Based on the equations of the three-dimensional elasticity theory in the Lagrangian description, a nonlinear theory of initially imperfect doubly curved sandwich shells has been developed. The theory encompasses a number of effects that are essential toward a reliable prediction of their static and dynamic response behavior. Special cases of practical significance have been also described.

As applications of the derived theory, the buckling and postbuckling of flat and circular cylindrical uniaxially compressed sandwich panels have been analyzed.

Among others, it was revealed that buckling results of flat/circular cylindrical panels based on this theory reasonably agree with the ones obtained experimentally. It was also shown that in the cases considered in the paper the beneficial behavior of sandwich curved panels consisting of larger buckling loads, as compared with their flat structure counterparts, is not deteriorated in the postbuckling range by the occurrence of the snapping phenomenon featuring strong intensities. This trend constitutes an important departure from the one generally featured by composite and noncomposite shells whose load-carrying capacity is strongly affected by the emergence of the snap-through phenomenon and is imperfection sensitive.

It is believed that the results of this work will be useful toward a more rational design of sandwich constructions used in today's and tomorrow's high technology.

Appendix: Strain-Displacement Relationships

Bottom Facings

$$ {}'\varepsilon_{11} = \xi_{1,1} + \eta_{1,1} + \tfrac{1}{2} v_{3,1}^2 + v_{3,1}\mathring{v}_{3,1} - v_3/R_1 \qquad (1 \rightleftarrows 2) \qquad \text{(A1)} $$

$$ {}'\gamma_{12} = \xi_{1,2} + \xi_{2,1} + \eta_{1,2} + \eta_{2,1} + v_{3,1}v_{3,2} + \mathring{v}_{3,1}v_{3,2} + v_{3,1}\mathring{v}_{3,2} \qquad \text{(A2)} $$

$$ {}'\gamma_{13} = {}'\psi_1 + v_{3,1} \qquad (1 \rightleftarrows 2) \qquad \text{(A3)} $$

$$ {}'\kappa_{11} = {}'\psi_{1,1} \qquad (1 \rightleftarrows 2) \qquad \text{(A4)} $$

$$ {}'\kappa_{12} = {}'\psi_{1,2} + {}'\psi_{2,1} \qquad \text{(A5)} $$

Core Layer

$$ \bar{\varepsilon}_{11} = \xi_{1,1} - \tfrac{1}{4}\left(h'\,{}'\psi_{1,1} - h''\,{}''\psi_{1,1}\right) + \tfrac{1}{2} v_{3,1}^2 + \mathring{v}_{3,1}v_{3,1} - v_3/R_1 \qquad (1 \rightleftarrows 2) \qquad \text{(A6)} $$

$$ \bar{\gamma}_{12} = \xi_{1,2} + \xi_{2,1} - \tfrac{1}{4}\left[h'\left({}'\psi_{1,2} + {}'\psi_{2,1}\right) - h''\left({}''\psi_{1,2} + {}''\psi_{2,1}\right)\right] $$
$$ + v_{3,1}v_{3,2} + \mathring{v}_{3,1}v_{3,2} + v_{3,1}\mathring{v}_{3,2} \qquad \text{(A7)} $$

$$ \bar{\kappa}_{11} = (1/\bar{h})\left\{\eta_{1,1} - \tfrac{1}{4}\left(h'\,{}'\psi_{1,1} + h''\,{}''\psi_{1,1}\right)\right\} \qquad (1 \rightleftarrows 2) \qquad \text{(A8)} $$

$$\bar{\kappa}_{12} = (1/\bar{h})\left\{\eta_{1,2} + \eta_{2,1} - \tfrac{1}{4}[h'(\psi'_{1,2} + \psi'_{2,1}) + h''(\psi''_{1,2} + \psi''_{2,1})]\right\} \tag{A9}$$

$$\bar{\gamma}_{13} = (1/\bar{h})\left\{\eta_1 - \tfrac{1}{4}(h'\psi'_1 + h''\psi''_1)\right\} + v_{3,1} \qquad (1 \rightleftarrows 2) \tag{A10}$$

Upper Facings

$$^{\prime\prime}\varepsilon_{11} = \xi_{1,1} - \eta_{1,1} + \tfrac{1}{2}(v_{3,1})^2 + \mathring{v}_{3,1}v_{3,1} - v_3/R_1 \qquad (1 \rightleftarrows 2) \tag{A11}$$

$$^{\prime\prime}\gamma_{12} = \xi_{1,2} + \xi_{2,1} - \eta_{1,2} - \eta_{2,1} + v_{3,1}v_{3,2} + \mathring{v}_{3,1}v_{3,2} + v_{3,1}\mathring{v}_{3,2} \tag{A12}$$

$$^{\prime\prime}\gamma_{13} = \psi''_1 + v_{3,1} \qquad (1 \rightleftarrows 2) \tag{A13}$$

$$^{\prime\prime}\kappa_{11} = \psi''_{1,1} \qquad (1 \rightleftarrows 2) \tag{A14}$$

$$^{\prime\prime}\kappa_{12} = \psi''_{1,2} + \psi''_{2,1} \tag{A15}$$

Acknowledgment

The work reported herein was supported in part by NASA Langley Research Center under Grant NAG 1-1689.

References

[1]Yu, Y. Y., "Nonlinear Flexural Vibrations of Sandwich Plates," *Journal of the Acoustical Society of America*, Vol. 34, No. 9, Pt. 1, 1962, pp. 1176–1183.

[2]Ebcioglu, I. K., "Nonlinear Theory of Sandwich Panels," *Developments in Theoretical and Applied Mechanics*, edited by Daniel Frederick, Vol. 4, Pergamon, Oxford, England, UK, 1970, pp. 611–637.

[3]Ebcioglu, I. K., "A General Theory of Sandwich Panels," *International Journal of Engineering Science*, Vol. 27, No. 8, 1989, pp. 865–878.

[4]Librescu, L., "On a Geometrically Non-Linear Theory of Elastic Anisotropic Sandwich-Type Plates," *Revue Roumaine des Sciences Techniques—Mecanique Appliquee*, Vol. 15, No. 2, 1970, pp. 323–339.

[5]Librescu, L., *Elastostatics and Kinetics of Anisotropic and Heterogeneous Shell-Type Structures*, Noordhoff International, Leyden, The Netherlands, 1975, Chaps. 5–7, pp. 493–540.

[6]Grigoliuk, E. I., "Large Deflection of Sandwich Shells with Strong Core," *Isvestia Academii; Nauk SSSR*, OTN, Vol. 1, 1958, pp. 26–34.

[7]Grigoliuk, E. I., and Chulkov, P. P., "General Large-Deflection Theory of Elastic Sandwich Shallow Shells," *Archiwum Mechaniki Stosowanej*, Vol. 1, No. 16, 1964, pp. 123–133.

[8]Kurshin, L. M., "Large Defelction of Sandwich Cylindrical Shells," *Research of Aeronautical Structures-Sandwich Plates and Shells*, edited by A. Ia. Alexandrov, Obornghiz, Moscow, 1959, pp. 39–50 (in Russian).

[9]Fulton, R. E., "Non-Linear Equations for a Shallow Unsymmetric Sandwich Shell of Double Curvature," *Developments in Mechanics, Proceedings of 7th Midwestern Mechanics Conference*, Plenum, New York, 1961, pp. 365–380.

[10]Noor, A. K., Burton, W. S., and Bert, C. W., "Computational Models for Sandwich Panels and Shells," *Applied Mechanics Reviews*, Vol. 4, No. 3, 1996, pp. 155–199.

[11]Librescu, L., "Refined Geometrically Non-Linear Theories of Anisotropic Laminated Shells," *Quarterly of Applied Mathematics*, Vol. 45, No. 1, 1987, pp. 1–22.

[12]Naghdi, P. M., "Foundations of Elastic Shell Theory," *Progress Solid Mechanics*, edited by I. N. Sneddon and R. Hill, Vol. 4, North-Holland, Amsterdam, The Netherlands, 1963, pp. 1–101.

[13]Meyer-Piening, H. R., "Remarks on Higher Order Sandwich Stress and Deflection Analysis," *Sandwich Constructions 1*, edited by K. A. Olsson and, R. P. Reichard, EMAS, Gradley Heath, Warley, England, UK, 1989, pp. 107–127.

[14]Vinson, J. R., *The Behavior of Shells Composed of Isotropic and Composite Materials*, Kluwer Academic, Norwell, MA, 1993.

[15]Librescu, L., and Stein, M., "A Geometrically Nonlinear Theory of Transversely-Isotropic Laminated Composite Plates and Its Use in the Post-buckling Analysis," *Thin Walled Structures, Special Aerospace Structures Issue*, Vol. 11, 1991, pp. 177–201.

[16]Librescu, L., and Stein, M., "Postbuckling Behavior of Shear Deformable Composite Flat Panels Taking Into Account Geometrical Imperfections," *AIAA Journal*, Vol. 30, No. 5, 1992, pp. 1352–1360.

[17]Librescu, L., and Chang, M. Y., "Post-Buckling and Imprefection Sensitivity of Shear Deformable Composite Doubly-Curved Panels," *International Journal of Solids and Structures*, Vol. 29, No. 9, 1992, pp. 1065–1083.

[18]Librescu, L., Lin, W., Nemeth, M. P., and Starnes, J. H., Jr., "Classical Versus Non-Classical Postbuckling Behavior of Laminated Composite Panels Under Complex Loading Conditions," *Non-Classical Problems of the Theory and Behavior of Structures Exposed to Complex Environmental Conditions*, edited by L. Librescu, AMD-Vol. 164, American Society of Mechanical Engineers, New York, 1993, pp. 169–182.

[19]Seide, P., "A Reexamination of Koiter's Theory of Initial Postbuckling Behavior and Imperfection Sensitivity of Structures," *Thin Shell Structures: Theory, Experiment and Design*, edited by C. Y. Fung and E. E. Sechler, Prentice–Hall, Englewood Cliffs, NJ, 1974, pp. 59–80.

[20]Librescu, L., "Aeroelastic Stability of Orthotropic Heterogeneous Thin Panels in the Vicinity of the Flutter Critical Boundary," *Journal de Mecanique*, Vol. 4, No. 1, 1965, pp. 51–76 (Pt. 1), and Vol. 6, No. 1, 1967, pp. 132–152 (Pt. 2).

[21]Palazotto, A. N., and Linneman, I. E., "Vibration and Buckling Characteristics of Composite Cylindrical Panels Incorporating the Effects of a Higher Order Shear Theory," *International Journal of Solids and Structures*, Vol. 28, No. 3, 1991, pp. 341–361.

[22]Alexandrov, A. I., Briuker, L. E., Kurshin, L. M., and Prusakov, A. P., *Research on Three-Layered Panels*, Oboronghiz, Moscow, 1960 (in Russian).

G. A. Kardomateas
Associate Editor